

## Effects of end distance on thin sheet steel bolted connections

Yancheng Cai <sup>a,\*</sup> and Ben Young <sup>b</sup>

<sup>a</sup> Department of Civil Engineering, The University of Hong Kong, Pokfulam Road, Hong Kong

<sup>b</sup> Department of Civil and Environmental Engineering, The Hong Kong Polytechnic University, Hong Kong  
(Formerly, Department of Civil Engineering, The University of Hong Kong, Pokfulam Road, Hong Kong)

### Abstract

The effects of end distance on thin sheet steel (TSS) bolted connections were investigated experimentally. The TSS grades G450, G500 and G550, with the respective nominal thicknesses of 1.90 mm, 1.20 mm and 0.42 mm, were used to fabricate the connection specimens. The connection specimens were assembled by one bolt in both single shear and double shear. The connection specimens in the single shear and double shear were designed in 5 series with different ratios of bolt diameter to connection plate thickness. In each series, the end distance of the connection specimen was varied. The connection specimens were subjected to tensile loading using the displacement control test method. The effects of end distance on the behavior of the specimens were obtained, including ultimate loads and failure modes. It was found that the ultimate loads were increased when the end distances were increased up to three times and five times the bolt diameter for single shear and double shear, respectively. Furthermore, the tearout failure mode progressed to bearing failure mode with the increment of the end distance. The experimental results were compared with the predicted nominal strengths and failure modes by using the Australian/New Zealand Standard (AS/NZS), North American Specification (NAS) and European Code (EC3-1.3) for cold-formed steel structures. Overall, it is found that both the NAS and EC3-1.3 specifications generally provide conservative predictions, while the AS/NZS generally provides unconservative predictions. However, the reliability analysis showed that the design provisions of AS/NZS are reliable and probabilistically safe for the TSS bolted connections in this study. The AS/NZS, NAS and EC3-1.3 generally predict accurate failure modes of the specimens. However, the EC3-1.3 provides more accurate predictions when specimens fail in plate bearing.

*Key words:* Bearing failure; bolted connection; end distance; thin-walled plates; tearout failure.

---

\* Corresponding author. Tel.: +852-2859-2665;

E-mail address: yccai@hku.hk (Y. Cai).

## 1. Introduction

Cold-formed steel structural members are normally fabricated from structural steel sheets by cold-rolling and brake-pressing methods [1], for examples, beams [2-3] (e.g., 0.48 mm G550 and 1.0 mm G500 in [3], where G550 and G500 are steel grades of 550 and 500 MPa with nominal 0.2% proof stresses, respectively) and columns [4-5] (e.g., 0.48 mm G550 and 1.0 mm G500). Structural steel sheets could also fabricate roof purlins [6], sandwich panels [7], profiled roofing sheets [8], members in portal frames [9] and roof trusses [10]. The thickness of the fabricated steel sheets in the construction could be less than 1.0 mm, for example, the thickness of brace member in the steel truss is 0.75 mm [10]. Structural members in cold-formed steel structures are commonly assembled by bolted connections in construction. Design rules for cold-formed steel bolted connections subjected to tensile loading are currently available in specifications [11-13]. The designs cover different failure modes of the bolted connections, including the failure modes in the connection plate such as bearing, tearout (shear rupture) and net section tension (tension rupture).

Rogers and Hancock [14] investigated 158 single shear (single overlap) bolted connection specimens assembled by thin sheet steels (TSS) at room (ambient) temperature condition that focused on the strength of the connection failure in the sheets, where TSS grade G550 with nominal thickness ( $t$ ) of 0.42 mm and 0.60 mm, and grade G300 with  $t$  of 0.60 mm were used to fabricate the specimens. Furthermore, another 18 specimens assembled by TSS 0.80 mm G550, 1.00 mm G550 and 0.80 mm G300, were tested to complement the aforementioned 158 tests [15]. Based on these findings, the Australian/New Zealand Standard (AS/NZS) [11] and North American Specification (NAS) [12] improved the bearing failure design of bolted connections. More recently, Yan and Young [16-18] conducted hundreds of experimental tests and numerical models on the effects of elevated temperatures on TSS (0.42 mm G550, 1.20 mm G500 and 1.90 mm G450) bolted connections. Subsequently, design rules were proposed for TSS bolted connections failure in the bearing of the sheets at elevated temperatures [18].

End distance ( $e_1$ ), i.e., the distance measured in the line of force from the center of the bolt hole to the nearest edge of an adjacent hole or to the end of the plate [11], has effects on the ultimate strength and failure mode of a bolted connection subjected to tensile loading. In a one-bolted connection specimen with sufficient connection plate width and bolt diameter ( $d$ ), the connection strength increases with the increment of  $e_1$  in a certain range, while the corresponding failure mode progresses from tearout to bearing in the connection plate. These have been reported in the one-bolted connections of cold-formed steel [19], structural steel [20] stainless steel [21-22] and more recently in high strength steel [23]. Teh and Uz [24] found that the equations for the ultimate shear-out (tearout) capacity of structural steel bolted connections in AISC Specification [25] lead to significant errors, while a more accurate equation was proposed. It should be noted that the effects of  $e_1$  on TSS bolted connections were investigated in specimens fabricated by 0.42 mm G550, 0.60 mm G550 and 0.60 mm G300 in single shear only [24], but there have been no investigations of TSS 1.20 mm G500 and 1.90 mm G450.

In this study, the effects of  $e_1$  on TSS single shear and double bolted connections were investigated experimentally. Three different grades of TSS, namely, 0.42 mm G550, 1.20 mm

G500 and 1.90 mm G450, were used to fabricate the connection specimens. The connection specimens in single shear and double shear were assembled by one bolt, and 5 series were designed with different ratios of  $d/t$ . In each series, the  $e_1$  of the connection specimens was varied. The connection specimens were subjected to tensile loading using the displacement control test method. The effects of  $e_1$  on the structural behavior of the specimens were obtained, i.e., load versus deflection curves, ultimate loads and failure modes. In addition, the experimental ultimate loads and failure modes were used to assess the accuracy of the predictions by design specifications for cold-formed steel structures, i.e., the AS/NZS [11], NAS [12] and European Code [13]. The reliability of the current design rules was evaluated using reliability analysis.

## 2. Coupon tests

The material properties of the three different grades of TSS, namely, 0.42 mm G550, 1.20 mm G500 and 1.90 mm G450, were measured using coupon tests. The TSS coupon specimens, having the respective gauge length and width of 25 mm and 6 mm, were cut in the rolling direction [16]. One coupon specimen was extracted from the steel sheets, and tested for each grade of TSS. Two strain gauges and a calibrated extensometer were used to measure the longitudinal strain of the specimen during the test. It should be noted that the zinc coating at the gauge length was removed in the coupon specimens. The coupon specimens were tested in an MTS tensile testing machine. The testing procedure suggested by Huang and Young [26] was adopted. Fig. 1 illustrates a close view of the test setup for the coupon tests. All the coupon specimens were fractured within the gauge length in the tests, i.e., within the measurements of the extensometer. The stress-strain curves of the three different grades of TSS are plotted in Fig.2. Table 1 summarizes the material properties of the TSS in this study, including Young's modulus ( $E$ ), longitudinal 0.2% proof stress ( $f_{0.2}$ ), longitudinal ultimate strength ( $f_u$ ), ultimate strain ( $\varepsilon_u$ ) and fracture strain ( $\varepsilon_f$ ). In addition, the average values of the measured width and thickness (after zinc coating removed) within the gauge length of the specimens were reported.

## 3. Bolted connection tests

### 3.1. General

Overall, 43 TSS bolted connection tests were conducted. The connection specimens were fabricated by the TSS 0.42 mm G550, 1.20 mm G500 and 1.90 mm G450. Each specimen was assembled by one bolt. The specimens were designed by varying the end distance ( $e_1$ ), namely, the value of  $e_1/d$  in this study. The tests were conducted by applying tensile loading at the specimen two ends with pin-end boundary conditions. The relationship between the applying load and the deflection, ultimate loads and failure modes of the specimen were obtained.

### 3.2. Specimen design and labeling

The TSS bolted connection specimens were designed in two types, single shear and double shear. A single bolt was used in each specimen. The single shear specimen was bolted with two identical TSS plates and the double shear with three identical TSS plates. However, the two external plates for double shear had a constant value of end distance  $e_1 = 4d$ . The connection plates were cut from the same batch of TSS as those for the coupon tests. The width ( $w$ ) of the connection plates was kept as 50 mm. The length ( $L$ ) of the connection plates was varied from 353 to 417 mm. The total length of 690 mm was maintained in the assembled specimens. The sizes of the bolt holes ( $d_o$ ) were standardized by following the AS/NZS [11] and NAS [12], where  $d_o = (d + 1)$  mm if  $d < 12$  mm, otherwise,  $d_o = (d + 2)$  mm is used. Grade 12.9 high strength steel bolts of different sizes were used, i.e., M6, M8 and M12. Washers at the two sides and nuts were used correspondingly. Fig. 3 illustrates the definition of symbols in the TSS plate. Tables 2-3 show the details of connection bolts and corresponding washers, respectively. The spacing requirements for a one-bolted connection specimen from different design specifications are illustrated in Table 4.

In each connection type, 5 different series were designed by using different sizes of  $d$ , as shown in Table 5. In each series, the value of  $e_1$  was varied, where  $e_1 = d, 2d, 3d$  and  $5d$  were designed for the single shear, and  $e_1 = d, 3d, 5d$  and  $6d$  were designed for the double shear. The larger values of  $e_1$  were designed for the double shear bolted connections compared with those for single shear bolted connections, e.g.,  $e_1 = 5d$  compared with  $e_1 = 3d$ . This is because for the same value of  $e_1$ , the bearing strengths of double shear are larger than those of the single shear, as reflected in the larger value of modification factor ( $m_f = 1.00$  for single shear and  $m_f = 1.33$  for double shear) is being used in the bearing strength calculation, e.g., AS/NZS [11] and NAS [12], which is illustrated in Section 4.2 of the present paper. Hence, the same value of  $e_1$  used enable pure plate bearing failure for single shear bolted connections, but may not guarantee the pure plate bearing failure for double shear bolted connections. The relatively larger values of  $e_1$  were designed for the double shear bolted connections such that the failure modes of the connection specimens progressed from pure plate tearout to pure plate bearing could be achieved, i.e., the effects of  $e_1$  in the failure modes from tearout to bearing. Similar design of larger  $e_1$  for plate bearing failure of double shear bolted connections at elevated temperatures was adopted by Yan and Young [19]. In the present study, the values of  $e_1$  were further increased for both single shear and double shear, e.g.,  $e_1 = 5d$  and  $e_1 = 6d$ , such that the effects of  $e_1$  on the connection strengths under the same failure mode could be investigated.

Each bolted connection specimen was labeled such that the  $t$  of the TSS, the connection type, the  $d$  and the  $e_1$  could be identified, as shown in Tables 6-7. For the examples of specimens “042-S-12-d” and 120-D-10-3d-r, the first segment indicates the  $t = 0.42$  mm for 042 and  $t = 1.20$  mm for 120 in the connection. The following segment means the connection type of single shear (S) and double shear (D). The third segment stands for the value  $d$  ( $d = 12$  mm and  $d = 10$  mm). The last part of the labeling indicates the  $e_1$  value ( $e_1 = d$  and  $e_1 = 3d$ ) in the connection. If it is a repeated test, the letter “r” is used in the last. Therefore, the bolted connection specimens were also identified in series with the last segment omitted, for example, Series 042-S-12 and Series 120-D-10.

### 3.3. Testing procedure

The experimental investigations of the TSS bolted connection specimens were carried out in an MTS machine. Figs. 4 and 5 illustrate the schematic view of the test setup for TSS single shear and double shear bolted connections, respectively. The elongation of the specimen was captured by the average readings of the two linear variable displacement transducers (LVDTs) during the test. The LVDTs were assembled in a frame that covered a distance of 200 mm in the middle part of the specimen. A length of 65 mm at each end of the specimen was assembled into the gripping apparatus. The specimen ends were fixed by the “fixed plate” and “adjustable plate” (see Figs. 4-5) by tightening the “bolts for fixing”. The gripping apparatus was designed such that the tensile loading was applied either through the shear plane of the specimens in single shear or concentrically loaded for the specimens in double shear [27]. The pin-ended boundary conditions of the gripping apparatus to the steel block were achieved by removing the “shanks” after tightening the “bolts for fixing”. The steel blocks were subsequently fixed to the grips of the testing machine. The descriptions of the test rig and operation for the bolted connections subjected to tensile loading are detailed in Cai and Young [27]. The curling up at the connection part was prevented by clips linked with iron wire [5, 7]. Tensile loading was applied onto the connection specimen by driving the actuator of the testing machine. The tests were conducted by displacement control with a constant rate of 1.0 mm/min. The applied load and the readings of LVDTs were recorded in a data acquisition system. Fig. 6 illustrates a typical test setup for a TSS double shear bolted connection.

### 3.4. Test results

The structural behavior of the TSS bolted connection specimens were obtained, including the relationship between the applied load and deflection during the tests, the ultimate loads ( $P_u$ ) and failure modes. Figs. 7-8 exemplify the load-deflection curves of TSS bolted connection for single shear Series 120-S-12 and double shear Series 120-D-12, respectively. The measured average deflection obtained by the two LVDTs for each specimen is plotted. The  $P_u$  of the connection specimens are shown in Tables 6-7 for single shear and double shear, respectively. The measured thicknesses ( $t_m$ ) of the specimens (with coating not removed) are also reported in the tables. The failure modes of the connection specimens are shown in Tables 8-9, for single shear and double shear, respectively. In the present study, the test failure modes include tearout failure (T) and bearing failure (B). Their characteristics are detailed by Rogers and Hancock [14], and by Yan and Young [18].

## 4. Design rules

### 4.1. General

Design rules for cold-formed steel bolted connections are provided in the current international specifications, including AS/NZS [11], NAS [12] and EC3-1.3 [13]. These

design rules are used to calculate the nominal strengths (unfactored design strengths) of the specimens in this study. Different failure modes are associated with the different design equations [11-13]. Hence, the minimum nominal strength is taken as the predicted strength of a bolted connection and, correspondingly, the predicted failure mode. A bolted connection specimen subjected to tensile loading may fail in the bolt by shear, or fail in the connection plate by bearing, tearout (shear rupture) or net section tension (tension rupture).

#### 4.2. Bearing failure

For bolted connection specimens that have failed in plate bearing, the nominal strength ( $P_b$ ) on each bolt in the AS/NZS [11] and the NAS [12] is re-written in Eqs. (1)-(2), where bolt hole deformation is considered:

$$P_b = C m_f d t_b f_u \quad (1)$$

$$C = \begin{cases} 3.0 & d/t_b < 10 \\ 4 - 0.1(d/t_b) & d/t_b \leq 22 \\ 1.8 & d/t_b > 22 \end{cases} \quad (2)$$

in which  $C$  is the bearing factor;  $m_f$  is the modification factor with  $m_f = 1.00$  for single shear and  $m_f = 1.33$  for double shear;  $t_b$  is the uncoated sheet (base metal) thickness. It should be noted that Eqs. (1)-(2) apply for  $0.42\text{mm} \leq t_b \leq 4.76\text{mm}$  in AS/NZS [11] and  $0.61\text{ mm} \leq t_b \leq 4.76\text{ mm}$  in NAS [12]. The TSS 0.42 mm G550 mm in this study is outside the range specified in NAS [12]. The NAS [12] is used for TSS 0.42 mm G550 mm as a direct comparison in this study. It should be noted that bearing strength with consideration of bolt hole deformation was not considered in the present study, e.g, the Eq. 5.3.4.3 in Section 5.3.4.3 of the AS/NZS [11] and the Eq. J3.3.2-1 in Section J3.3.2 of the NAS [12].

In EC3-1.3[13], the  $P_b$  is calculated by the following Eqs. (3)-(4):

$$P_b = 2.5 \alpha_b k_t f_u d t \quad (3)$$

$$k_t = \begin{cases} (0.8t + 1.5)/2.5 & 0.75\text{mm} \leq t \leq 1.25 \\ 1.0 & t > 1.25\text{mm} \end{cases} \quad (4)$$

where  $\alpha_b$  is the smallest of 1.0 or  $e_1/(3d)$ ;  $k_t$  is the modification factor. It should be noted that TSS 0.42 mm G550 in this study is also outside the range in the calculation of  $k_t$ . The  $(0.8t+1.5)/2.5$  was used to calculate the value of  $k_t$  for TSS 0.42 mm G550.

#### 4.3. Tearout failure

The tearout failure occurs with inadequate length of  $e_1$ . The nominal strength ( $P_{tear}$ ) for the tearout failure on each bolt specified in AS/NZS [11] is shown in Eq. (5). In NAS [12], the calculation of  $P_{tear}$  refers to shear rupture failure in Section J6.1 [12], and it is re-written in Eq. (6), in which  $A_{nv}$  is the net area subject to shear (parallel to force). The calculation of

$A_{nv}$  equals to  $2nte_{net}$ , where  $n$  is the number of fasteners on the critical cross-section;  $e_{net}$  is the clear distance between the end of the material and the edge of the fastener hole. It should be noted that AS/NZS [11] takes into consideration the  $e_l$  with coefficient of 1.0, while the NAS [12] considers  $e_{net}$  ( $e_{net} = e_l - d_o/2$ ) with the coefficient of 1.2, as shown in Eqs. (5) and (6).

$$P_{tear} = e_1 t_b f_u \quad (5)$$

$$P_{tear} = 0.6A_{nv}f_u = 1.2e_{net}t_b f_u \quad (6)$$

#### 4.4. Net section tension failure

For net section tension failure, the nominal strength ( $P_{net}$ ) is specified in Clause 3.2.2 and Clause 5.3.3 of the AS/NZS [11], where the nominal strength is determined by the minimum calculated from Eqs. (7)-(9).

$$P_{gr} = A_g f_y \quad (7)$$

$$P_{net} = 0.85k_1 A_n f_u \quad (8)$$

$$P_{net} = (0.9 + (0.1d/s_f))A_n f_u \quad (9)$$

where  $P_{gr}$  is the nominal section capacity of a member in tension;  $A_g$  is the gross area of the cross-section;  $f_y$  is the yield stress used in design, and  $f_y = f_{0.2}$  in this study;  $k_1$  is the correction factor for distribution of forces, and  $k_1 = 1.0$  in the present study;  $A_n$  is the net area of the cross-section;  $s_f$  is spacing of bolts perpendicular to the line of the force or width of sheet, in the case of a single bolt. In NAS [12], the nominal strength of net section tension failure refers to the calculation of tension rupture failure as specified in Section J6.2. The calculation is the same as Eq. (9) shown above. However, it should be noted that the NAS [12] does not require the calculation of Eq. (8).

In EC3-1.3 [13], the  $P_{net}$  is calculated according to Eq. (10) in addition to Eq. (7) shown above:

$$P_{net} = (1 + 3r(d_o/u - 0.3))A_n f_u \quad (10)$$

where  $r = (\text{number of bolts at the cross-section}) / (\text{total number of bolts in the connection})$ , and  $r = 1.0$  in the present study;  $u$  equals the width of the connection sheet.

## 5. Effects of end distance

### 5.1. Ultimate loads

The effects of  $e_l$  on the  $P_u$  of the TSS bolted connections were investigated. Figs. 9-10 plot the  $P_u$  against the variations of  $e_l/d$  for the connections in single shear and double shear,

respectively. For the single shear (see Fig. 9), it is shown that the  $P_u$  increase obviously with the increment of  $e_1/d$  from 1 to 3 for each series. The increments of  $P_u$  are larger from  $e_1/d = 1$  to  $e_1/d = 2$  than from  $e_1/d = 2$  to  $e_1/d = 3$ . The  $P_u$  are generally maintained when the values of  $e_1/d$  increase from 3 to 5. Similarly for the double shear (see Fig. 10), the  $P_u$  increase obviously with the values of  $e_1/d$  increase from 1 to 5 for each series. The increments of  $P_u$  are larger from  $e_1/d = 1$  to  $e_1/d = 3$  than from  $e_1/d = 3$  to  $e_1/d = 5$ . The  $P_u$  are generally maintained when the values of  $e_1/d$  increase from 5 to 6. This may indicate that for TSS single shear bolted connections, the  $P_u$  are generally maintained when the  $e_1 \geq 3d$ , while for the double shear bolted connections, the  $e_1 = 3d$  is not enough to maintain the ultimate loads. This will be discussed further in the later section. Note that bolt shear failure and net section tension failure were deliberately avoided in the specimen designs, and not found in the test results.

## 5.2. Failure modes

The failure modes of the connection specimens are shown in Tables 9-10, for single shear and double shear, respectively. For the single shear (see Table 9), all the connection series failed in tearout (T) with  $e_1/d = 1$  and  $e_1/d = 2$ . The tearout failure mode was not found when  $e_1$  was increased to  $3d$ ; instead, the bearing failure (B) mode took over. The specimens failed in the same bearing failure when  $e_1$  was increased from  $3d$  to  $5d$ . For the double shear (see Table 10), the specimens failed obviously in tearout with  $e_1$  equaled to  $d$ , and such failure mode was not that obvious when the  $e_1$  was increased to  $3d$ , where the splitting of material at the end of the plates occurred. This phenomenon of splitting at the end of the plates at a relatively smaller value of  $e_1$  was also found in Wang *et al.* [23] for double shear bolted connections assembled by high strength steel plates. The characteristics of tearout or splitting of material at the end of the plates were not observed for  $e_1 = 5d$  and  $e_1 = 6d$ . Instead, pure bearing failure mode was observed. Figs. 11-15 illustrate the failure modes of specimen series 120-S-10, 190-S-10, 042-D-12, 120-D-12 and 190-D-10, respectively.

## 5.3. Single shear and double shear

The ultimate strengths and failure modes of TSS bolted connections between single shear specimens and double shear specimens for the same bolt hole and end distance are investigated. In the present study, all the connection specimens were designed with one bolt hole. Fig. 16 plots the normalized values of ultimate strength against the end distance in terms of  $e_1/d$ . The normalized values in the vertical axis were obtained by dividing the ultimate strengths of double shear bolted connections with those of the single shear bolted connections, which is normalized by the ultimate strengths of single shear bolted connections. The labeling systems for the specimens described in Section 3.2 of this paper were adopted for the legends in the figure, but simplified to distinguish the plate thickness and bolt diameter, e.g., 042-12. It was found that for the same end distance of  $e_1/d$ , the strengths of double shear are generally higher than those of single shear, as evident by the normalized values greater than 1.0. As the end distance increases, e.g., from  $e_1/d = 1.0$  to  $e_1/d = 5.0$ , the normalized values are getting larger, from the maximum of 1.09 for  $e_1/d = 1.0$  to the

maximum of 1.43 for  $e_1/d = 5.0$ . In addition, it is shown that for the lower values of  $d/t$ , the normalized values increase more obviously as the end distance of  $e_1/d$  increases, e.g., the increment of 042-12 with  $d/t = 25.6$  increased from 1.09 to 1.18, compared with that of 120-12 with  $d/t = 6.7$  increased from 0.99 to 1.43. While for the failure modes of the single shear and double shear bolted connections, the pure tearout failure mode was found for both single shear and double shear when  $e_1/d = 1.0$ . The failure mode progressed to pure bearing as  $e_1/d$  increased from 1.0 to 3.0 for single shear bolted connections; while the tearout failure mode still exists for double shear bolted connections as  $e_1/d$  increased from 1.0 to 3.0, as described previously in Section 5.2 of the present paper. This indicates that the end distance of  $e_1/d = 3.0$  is sufficient to obtain pure bearing failure mode for single shear bolted connections, but may not be the case for double shear bolted connections, which were explained in the specimen design in Section 3.2 and illustrated by the modification factors in the bearing strength design in Section 4.2 of this paper. However, the pure bearing failure was obtained for both single shear and double shear bolted connections when  $e_1/d$  was further increased to 5.0.

## 6. Comparison of test results with predictions

### 6.1. General

The experimental results were compared with the predicted results using the cold-formed steel design specifications [11-13] in terms of connection strengths and failure modes. In the calculation of predicted strengths, the aforementioned design equations in Section 4 of this paper were used. It should be noted that, in Clause 1.5.1.1 of AS/NZS [11], it is stated that for steel Grade 550, if the thickness is less than 0.6 mm, the use of  $f_{0.2}$  and  $f_u$  are taken as 90% of the corresponding specified values or 410 MPa, whichever is the lesser. In NAS [12], for steels with  $3\% \leq \text{elongation} < 10\%$  as specified in the Section A3.1.2 [12], a reduced yield stress of  $0.9f_{0.2}$  and the tensile strength of  $0.9f_u$  should be used in place of  $f_{0.2}$  and  $f_u$ , respectively; and for steels with  $\text{elongation} < 3\%$  as specified in the Section A3.1.3 [12], the use of  $f_{0.2}$  is taken as the lesser of  $0.75f_{0.2}$  and 414 MPa; and the use of  $f_u$  is taken as the lesser of  $0.75f_u$  and 427 MPa. Note that the EC3-1.3 [13] does not specify the reduced values of  $f_{0.2}$  and  $f_u$  in the calculations.

The obtained material properties (see Table 1) of the three different grades of TSS and the measured thicknesses ( $t_m$ ) of the connection specimens were used in the calculation. However, the nominal thickness of steel 0.42 mm G550 is less than 0.6 mm, hence, the aforementioned Clause 1.5.1.1 of AS/NZS [11] was followed, and the value of 410 MPa was adopted. The steel 1.20 mm G500 had an elongation of 9.2% (see Table 1) which was within  $3\% \leq \text{elongation} < 10\%$  and steel 0.42 mm G550 had an elongation of 2.9% (see Table 1), less than 3%. Hence, the aforementioned rules specified in sections A3.1.2 and A3.1.3 of NAS [12] were also followed in the calculations. The values of  $0.9f_{0.2}$  and  $0.9f_u$  were used for steel 1.20 mm G500; while the values of 414 MPa and 427 MPa were adopted for  $f_{0.2}$  and  $f_u$  of steel 0.42 mm G550, respectively. For the purpose of direction comparison, the obtained material properties without reductions were also used in the calculation.

## 6.2. Comparison of test and predicted strengths

The predicted strength was determined by the minimum nominal strength of a bolted connection by considering different failure modes [11-13]. Note that bolt shear failure was deliberately avoided in the specimen design, and this failure mode was not observed in the test results. Tables 6-7 show the comparisons between the  $P_u$  and the predicted strengths for the single shear and double shear, respectively. The predicted strengths by using the reduced material properties were also obtained and compared, where the results are bracketed as shown in Tables 6-7. Table 8 summarizes the comparison of the TSS bolted connections, where the un-reduced material properties were used as a direct comparison.

For TSS single shear bolted connections (see Table 6), both the NAS [12] and EC3-1.3 [13] generally provide conservative predictions for all the series of connections, while the predictions by EC3-1.3 [13] are less conservative and less scattered, e.g., the mean values of  $P_u/P_{NAS}$  and  $P_u/P_{EC}$  for steel 1.20 mm G500 are 1.10 and 1.02 with the corresponding coefficient of variation (COV) of 0.312 and 0.089. When the reduced material properties are used, the NAS [12] provides more conservative predictions, e.g., the  $P_u/P_{NAS}$  increases from 1.14 to 1.98 for steel 0.42 mm G550. It was found that the AS/NZS [11] provides unconservative predictions for all the series of connections, as the mean values of  $P_u/P_{AS/NZS}$  are smaller than 1.00. However, the predictions become very conservative when the reduced material properties are used, e.g., the mean of  $P_u/P_{AS/NZS}$  increases from 0.93 to 1.68 for steel 0.42 mm G550. As summarized in Table 8, it was found that the EC3-1.3 [13] provides less conservative and less scattered nominal strength predictions than NAS [12], while the AS.NZS [11] provides un-conservative predictions.

For double shear bolted connections (see Table 7), both the NAS [12] and EC3-1.3 [13] generally provide conservative predictions for all the connection series. However, the NAS [12] provides less conservative but more scattered predictions, e.g., the mean values of  $P_u/P_{NAS}$  and  $P_u/P_{EC}$  for steel 0.42 mm G550 are 1.02 and 1.14 with the corresponding COV of 0.375 and 0.126. Similar to the single shear, the NAS [12] provides more conservative predictions when the reduced material properties are used; e.g., the mean value of  $P_u/P_{NAS}$  increases from 1.09 to 1.21 for steel 1.20 mm G500. The AS/NZS [11] generally provides unconservative predictions for all the series of connections when the unreduced material properties are used. However, the predictions become very conservative when the reduced material properties are used, e.g., the mean value of  $P_u/P_{AS/NZS}$  increases from 0.85 to 1.54 for steel 0.42 mm G550. As summarized in Table 8, it was found that the NAS [12] provides less conservative but more scattered nominal strength predictions than EC3-1.3 [13], while the AS.NZS [11] provides un-conservative predictions.

As mentioned in Section 5.2, the test failure modes of the TSS connection specimens included tearout and bearing failure modes only. The strengths calculation for the failure modes of tearout and bearing are related closely to the parameters of  $t$ ,  $f_u$ ,  $d$  and  $e_1/d$ , as shown in Eqs. (1)-(6). Therefore, the factors of  $P_u/f_u dt$  for the TSS connection specimens were calculated, where the unreduced material properties of  $f_u$  (see Table 1) were used. The relationships between the  $P_u/f_u dt$  and  $e_1/d$  for each specimen are shown in Figs. 17-18, for single shear and double shear, respectively. The curves predicted by the design equations from the specifications [11, 13] are also shown. It should be noted that, in the calculation of

Equation (4), the average measured values of 0.47 mm for TSS 0.42 mm G550 were used instead of using the nominal thickness of 0.42 mm. The nominal ratios of  $d/t$  for each specimen series are also indicated, with the actual values of  $d/t_m$  shown in Tables 6-7. The curves of NAS [3] were not plotted as the value of  $e_{net}$  ( $e_{net} = e_1 - d_o$ ) in Eq. (6) for the shear fracture (tearout) was not related directly to  $d$ , due to the subtraction of  $d_o$  in the calculation. However, it should be noted that the design equations for bearing failure in NAS [12] and AS/NZS [11] are the same (see Eq. (1)-(2)). As shown in Figs. 17-18, the EC3-1.3 [13] (dotted lines with black color) gives better predictions than AS/NZS [11] (solid lines with red color) for the trends of  $P_u/f_u dt$  with the increment of  $e_1/d$ .

### 6.3. Reliability analysis

Reliability analysis was performed for the TSS bolted connection design rules used in this study. The analysis was conducted in accordance with those specified in the North American Specification (NAS) for the Design of Cold-Formed Steel Structural Members [12]. The aforementioned bolted connection design provisions in the AS/NZS [11], NAS [12] and EC3-1.3 [13] as specified in Section 5.2 of this paper were examined. It should be noted that Section A.6 of the EC3-1.3 [13] provides the procedure for evaluation of test results. For direct comparison, the reliability analysis that specified in the NAS [12] was used in this study.

In the present study, the reliability index ( $\beta$ ) greater than or equal to 3.5 as specified in Section K2.1 of the NAS [12] was set for the design provisions being considered reliable and probabilistically safe. The resistance factors ( $\phi$ ) for bolted connection strength design as recommended by the AS/NZS [11], NAS [12] and EC3-1.3 [13] are shown in Table 8. They were used in the calculation of the reliability index ( $\beta$ ). It should be noted that different resistance factors are specified for bolted connections subjected to different failure modes [11-12], e.g., 0.6 and 0.9 for the failure modes of bearing and net section tension, respectively [11]. The resistance factor of 0.6 was used in the reliability analysis for both AS/NZS [11] and NAS [12]. This is because the present study mainly focused on the TSS bolted connections subjected to failure of tearout and bearing, which are also the main failure modes predicted by AS/NZS [11] and NAS [12], as detailed in Section 6.4 of this paper. The resistance factor of 0.8, which is  $1/1.25$ , was used for EC3-1.3 [13]. This resistance factor is specified in Table 8.4 of the EC3-1.3 [13] for different failure modes of bolted connections. In addition, the load combinations of  $1.2DL + 1.5LL$  [28],  $1.2DL + 1.6LL$  [12] and  $1.35DL + 1.5LL$  [29] were used for the design provisions of AS/NZS [11], NAS [12] and EC3-1.3 [13], respectively; where DL represents the dead load while LL represents the live load. The ratio of 0.2 was used for DL/LL. The statistical parameters suggested in Section 6.2 of the NAS [12] were used, where  $M_m = 1.10$ ,  $F_m = 1.00$ ,  $V_M = 0.08$  and  $V_F = 0.05$ , which are the mean values and coefficients of variation of material factor and fabrication factor, respectively. In addition, the mean value ( $P_m$ ) and the coefficients of variation ( $V_P$ ) of tests to the design prediction ratios (used unreduced material properties) are shown in Table 8. A correction factor ( $C_P$ ) in the Section K2.1 of the NAS [12] was used to take into consideration of the influence of limited number of test data, where  $C_P = (1+1/n)m/(m-2)$ , in which  $n$  is the number of tests and  $m = n-1$  is the degrees of freedom. The reliability index ( $\beta$ ) for the TSS

single shear and double shear bolted connections were calculated, and reported in Table 8.

It was found that the design provisions of AS/NZS [11] are reliable and probabilistically safe for TSS bolted connections in both single shear and double shear, as evident by the value of  $\beta$  not less than 3.5, except for single shear where  $\beta = 3.49$  which is very close to the target value of 3.5. On the contrary, the design provisions of NAS [12] and EC3-1.3 [13] are not reliable and probabilistically not safe due to the smaller values of  $\beta$  ( $< 3.5$ ), although it has been shown that the predictions by NAS [12] and EC3-1.3 [13] are generally conservative with the mean values of test to predictions greater than 1.0. This may be due to the relatively large values of COV in the predictions [12-13], e.g., 0.287 and 0.309 for single shear and double shear, respectively, for NAS [12]. For the purpose of direct comparison, a constant resistance factor of 0.60 and a load combination of 1.2DL +1.6LL as specified in the NAS [12] were used to calculate the reliability index ( $\beta$ ), as shown in (x)\* in Table 8. It is shown that the design provisions of AS/NZS [11] are more reliable and probabilistically safe due to the increased values of  $\beta$ . The design provisions of EC3-1.3 [13] become reliable and probabilistically safe, this is mainly due to the resistance factor was reduced from 0.80 to 0.60.

#### 6.4. Comparison of test and predicted failure modes

The failure mode associated with the minimum nominal strength for each specimen was taken as the predicted failure mode. Tables 9-10 show the predicted failure modes for single shear and double shear, respectively. It should be noted that the effect of  $e_1$  on the bolted connection strength is incorporated into the strength calculation of bearing failure by the coefficients of  $\alpha_b$  (see Eq. (3)) in the EC3-1.3 [13], hence, EC3-1.3 [13] does not distinguish the tearout failure and bearing failure, but predicts the two failure modes as bearing failure. However, the AS/NZS [11] and NAS [12] provide tearout (shear fracture) failure and bearing failure modes.

For TSS single shear, it was found that the AS/NZS [11] is able to predict the failure modes correctly, except for specimens 042-S-12-2d, 120-S-12-3d and 120-S-12-5d. For Specimen 042-S-12-2d, the bearing failure was predicted but the test specimen failed in tearout. This is because the value of  $C = 1.8$  (see Eq. (2)) for  $d/t_m = 25.53$  (see Table 6) was used in the calculation of  $P_b$ ; while for Specimen 120-S-12-2d with  $d/t_m = 8.06$  (see Table 6) that having the same  $e_1 = 2d$  but different thickness, the value of  $C = 3.0$  (see Eq. (2)) was used, hence, the calculated result of  $P_b$  became larger; it was also larger than the value of  $P_{tear}$ . Therefore, the predicted failure mode of Specimen 120-S-12-2d was tearout instead of bearing, as shown in Table 9. The smaller values of bearing factor  $C$  due to the larger ratios of  $d/t_m$  (see Eqs. (1)-(2)) would yield smaller predictions of  $P_b$ . This also explains the fact that, for the specimens with the same  $e_1$  but different  $d/t_m$ , the bearing failure mode was predicted for specimens 042-S-12-3d and 042-S-12-5d, but the net section tension failure mode for specimens 120-S-12-3d and 120-S-12-5d. For specimens 120-S-8-3d, 120-S-10-3d and 190-S-10-3d, the nominal strengths of  $P_b$  and  $P_{tear}$  were the same; hence, the predictions included the two failure modes. The NAS [12] shares the same equations for the calculation of  $P_b$  as those in AS/NZS [11]. However, for the calculation of  $P_{tear}$ , the NAS [12] takes into consideration  $e_{net}$  with a coefficient of 1.2 (see Eq. (6)) instead of  $e_1$  with a coefficient of 1.0

(see Eq. (5)), which generally yields a lower nominal strength of  $P_{tear}$ . This explains the tearout failure prediction by NAS [12] for specimens 120-S-8-3d, 120-S-10-3d and 190-S-10-3d. Net section tension failure mode was not predicted by EC3-1.3 [13], which was consistent with the test results.

For the TSS double shear, AS/NZS [11] and NAS [12] provided the same failure modes for all the specimens. Similar to the effects of factor  $C$  associated with  $d/t_m$  in single shear, bearing failure was predicted for specimen Series 042-D-12 compared to the net section tension failure prediction for specimen Series 120-D-12, for the same  $e_1$  of 3d, 5d and 6d. The net section tension failure was predicted for specimen series 120-D-10 and 190-D-10 with end distances of 5d and 6d, which was different from the predictions in single shear. This is because a larger  $P_b$  is obtained by the coefficient of  $m_f = 1.33$  for double shear compared to  $m_f = 1.00$  for single shear in the calculation ((see Eq. (1)). Similar to the single shear, net section tension failure mode was not predicted by EC3-1.3 [13], which is consistent with the test results.

## 7. Conclusions

Totally 43 specimens were designed and tested to investigate the effects of end distance ( $e_1$ ) on thin sheet steel (TSS) bolted connections. The connection specimens were fabricated by three different grades of TSS, namely, 0.42 mm G550, 1.20 mm G500 and 1.90 mm G450. The TSS connection specimens were assembled by one bolt in two types, i.e., single shear and double shear. The connection type was designed in 5 series with different ratios of bolt diameter ( $d$ ) to plate thickness ( $t$ ). In each specimen series, the value of  $e_1$  was varied. The connection specimens were subjected to tensile loading by the displacement control test method. The effects of  $e_1$  on the ultimate loads ( $P_u$ ) and failure modes of the specimens were obtained. Findings from the experimental investigations are summarized below:

- It was found that the  $P_u$  of bolted connections increased when  $e_1$  increased from  $d$  to  $3d$  for the single shear bolted connections; and from  $d$  to  $5d$  for the double shear bolted connections.
- The  $P_u$  was generally maintained approximately the same value when the  $e_1$  increased from  $3d$  to  $5d$  for the single shear bolted connections; and from  $5d$  to  $6d$  for the double shear bolted connections.
- It is shown that  $e_1 = 3d$  could prevent the tearout failure in single shear bolted connections, while  $e_1 > 3d$  is suggested to prevent the tearout failure in double shear bolted connections.
- As the end distance increases, the strength increments for double shear are higher those of single shear bolted connections, i.e., from  $e_1/d = 1.0$  to  $e_1/d = 5.0$ . In addition, for the lower values of  $d/t$ , more increments of connection strengths were obtained as the end distance of  $e_1/d$  increased.

The test results were compared with the predicted results calculated by the current design rules in terms of strengths and failure modes. The reliability of the current design rules was evaluated using reliability analysis. The specifications for cold-formed steel structures

were used for the predictions, i.e., Australian/New Zealand Standard (AS/NZS) [11], North American Specification (NAS) [12] and European Code (EC3-1.3) [13]. Findings of the comparisons are summarized below:

- Overall, it was found that both the NAS [12] and EC3-1.3 [13] specifications generally provide conservative predictions, while the AS/NZS generally provide unconservative predictions.
- However, the design provisions of AS/NZS [11] are reliable and probabilistically safe for the TSS bolted connections in both single shear and double shear due to the relatively small values of coefficient of variation.
- Generally, the AS/NZS [11] and NAS [12] provided accurate predictions for the failure modes of the specimens.

### **Acknowledgments**

The authors are grateful to BlueScope Lysaght (Singapore) Pte. Ltd. for supplying the test specimens. The research work described in this paper was supported by a grant from the Research Grants Council of the Hong Kong Special Administrative Region, China (Project No. HKU719711E).

### **References**

- [1] Yu W.W. Cold-formed steel design. 3rd ed.. New York: Wiley; 2000.
- [2] Wang, L.P., Young, B. "Behavior of Cold-Formed Steel Built-Up Sections with Intermediate Stiffeners under Bending. II: Parametric Study and Design." *Journal of Structural Engineering* 2016, 142(3), 04015151-1-11.
- [3] Laím, L., Rodrigues, J.P.C., and da Silva, L.S. "Experimental and numerical analysis on the structural behaviour of cold-formed steel beams." *Thin-Walled Structures* 2013, 1–13.
- [4] Zhang J.-H., Young B. Experimental investigation of cold-formed steel built-up closed section columns with web stiffeners *Journal of Constructional Steel Research* 2018, 147, 380–392.
- [5] Zhang J.-H., Young B.. Numerical investigation and design of cold-formed steel built-up open section columns with longitudinal stiffeners. *Thin-Walled Structures* 2015, 89, 178–191.
- [6] Congxiao Zhao, Jian Yang, Feiliang Wang and Andrew H.C. Chan. Rotational stiffness of cold-formed steel roof purlin–sheeting connections. *Engineering Structures* 2014, 59, 284–297.
- [7] Yasser A. Khalifa, Wael W. El-Dakhkhni, Manuel Campidelli and Michael J. Tait. Performance assessment of metallic sandwich panels under quasi-static loading. *Engineering Structures* 2018, 158, 79–94.
- [8] Xu Y. L., Reardon G. F. Test of screw fastened profiled roofing sheets subject to simulated wind uplift. *Engng Struct.* 1993, 15(6), 423-430.
- [9] Lim J. B. P., D. A. Nethercot. Design and development of a general cold-formed steel

portal framing system. *The Structural Engineer*. November, 2002, 31-40.

[10] Yuanqi Li, Zuyan Shen, Xingyou Yao, Rongkui Ma and Fei Liu. Experimental Investigation and Design Method Research on Low-Rise Cold-Formed Thin-Walled Steel Framing Buildings. *Journal of Structural Engineering* 2013, 139(5): 818-836.

[11] AS/NZS 4600, Cold-formed Steel Structures, Australian/New Zealand Standard, AS/NZS4600:2018, Sydney, Australia, Standards Australia, 2018.

[12] NAS, North American Specification for the Design of Cold-Formed Steel Structural Members, American Iron and Steel Institute, AISIS100-2016, AISI Standard, 2016.

[13] EC3-1.3, Eurocode3—Design of Steel Structures—Part 1–3: General Rules Supplementary Rules for Cold-formed Members and Sheeting. Brussels: European Committee for Standardization, EN1993-1-3:2006, 2006.

[14] Rogers CA, Hancock GJ. Bolted connection tests of thin G550 and G300 sheet steels. *Journal of Structural Engineering* 1998;124(7):798–808.

[15] Rogers CA, Hancock GJ. Bolted connection design for sheet steels less than 1.0 mm thick. *Journal of Constructional Steel Research* 1999;123–4651 1999:123–46.

[16] Yan S, Young B. Tests of single shear bolted connections of thin sheet steels at elevated temperatures - Part I: steady state tests. *Thin-Walled Structures* 2011; 49:1320–33.

[17] Yan S, Young B. Effects of Elevated Temperatures on Double Shear Bolted Connections of Thin Sheet Steels. *Journal of Structural Engineering* 2013; 139: 757-771.

[18] Yan S, Young B. Bearing factors for single shear bolted connections of thin sheet steels at elevated temperatures. *Thin-Walled Structures* 2012; 52:126–142.

[19] Seleim S. and LaBoube R. Behavior of low ductility steels in cold-formed steel connections, *Thin-Walled Structures* 1996, 25(2), 135-151.

[20] Kim H.J. and Yura J.A. The effect of ultimate-to-yield ratio on the bearing strength of bolted connections, *Journal of Constructional Steel Research* 1999, 49: 255-269.

[21] Salih, E.L., Gardner L., and Nethercot D.A. Bearing failure in stainless steel bolted connections, *Engineering Structures* 2011; 33(2): 549–562.

[22] Cai Y. and Young B. Bearing Factors of Cold-formed Stainless Steel Double Shear Bolted Connections at Elevated Temperatures, *Thin-walled Structures* 2016, 9, 212-219.

[23] Wang Y-B, Lyu, Y-F, Li G-Q and Liew J.R.R. Behavior of single bolt bearing on high strength steel plate, *Journal of Constructional Steel Research* 2017, 137: 19-30.

[24] Teh L.H. and Uz M.E. Ultimate shear-out capacities of structural-steel bolted connections, *Journal of Structural Engineering* 2015; 141(6): 04044152-9.

[25] AISC, Specification for structural steel buildings, American Institute of Steel Construction, ANSI/AISC 360-10, Chicago, 2010.

[26] Huang Y. and Young B. The art of coupon tests. *Journal of Constructional Steel Research* 2014, 96: 159-175.

[27] Cai, Y. and Young, B. Structural behavior of cold-formed stainless steel bolted connections. *Thin-Walled Structures* 2014, 83: 147-156.

[28] AS/NZS 1170. Structural design actions. Part 0: General principles. Australian/New Zealand Standard, AS/NZS 1170.0:2002, Standards Association of Australia, Sydney, Australia.

[29] EC0. Eurocode 0: basis of structural design. EN 1990:2002+A1:2005. Brussels, Belgium: European committee for standardization, 2005.

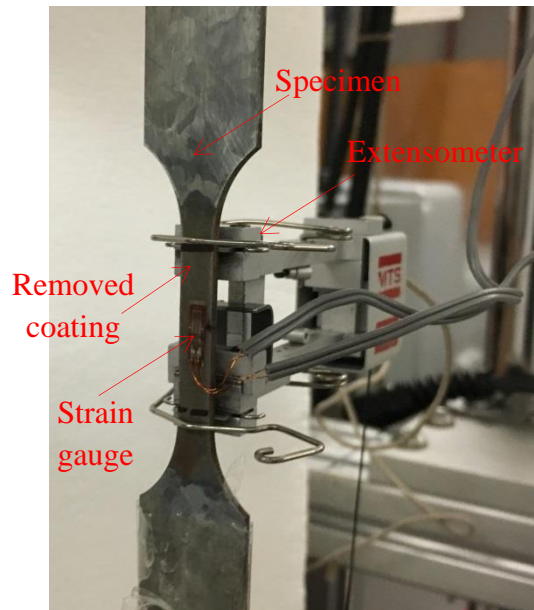


**Fig. 1.** Coupon test

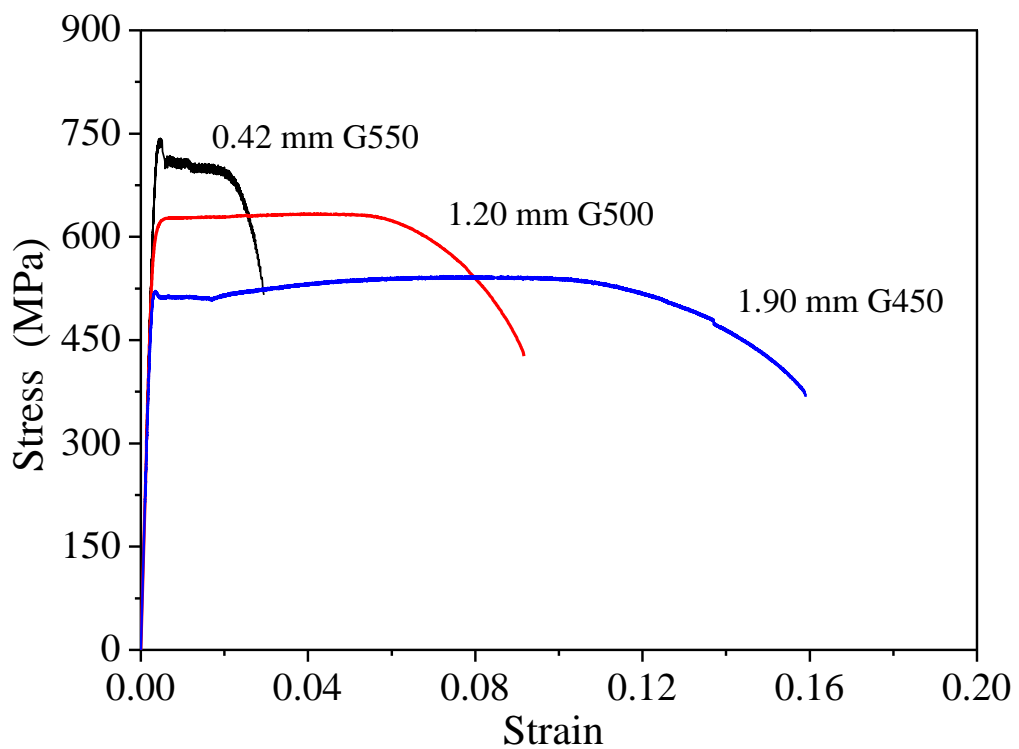


**Fig. 2.** Stress-strain curves of different grades of thin sheet steel

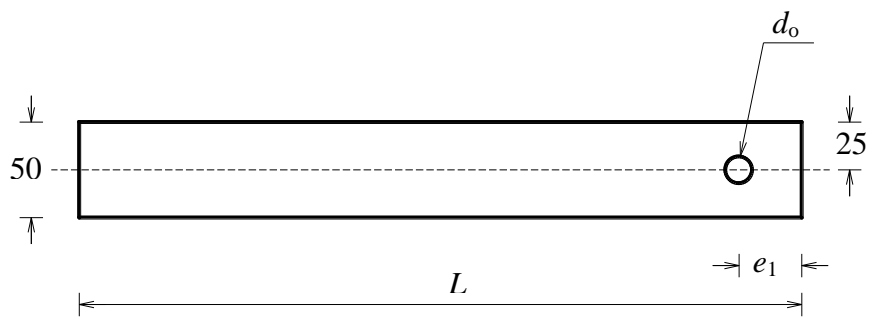


**Fig. 3.** Definition of symbols

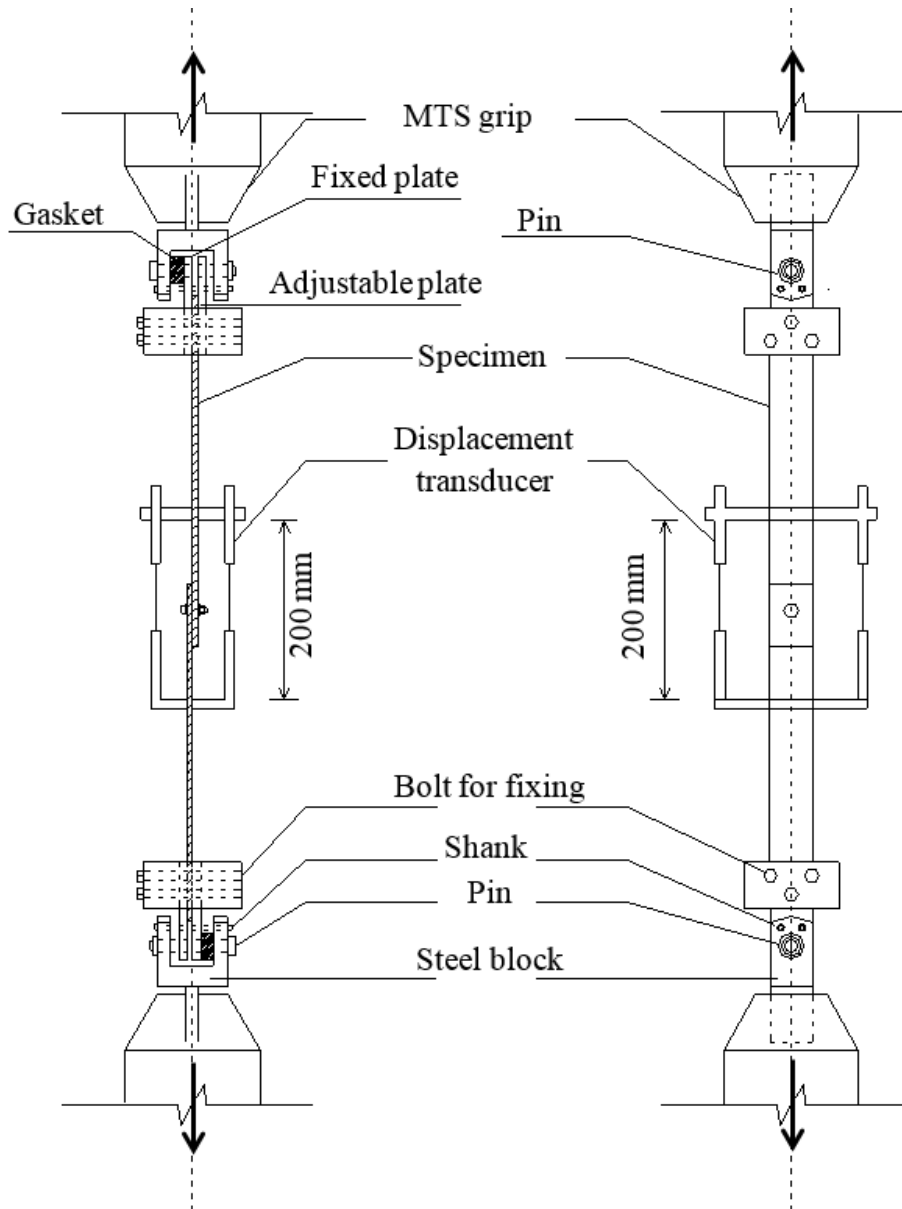


**Fig. 4.** Schematic view of test setup for TSS single shear bolted connection

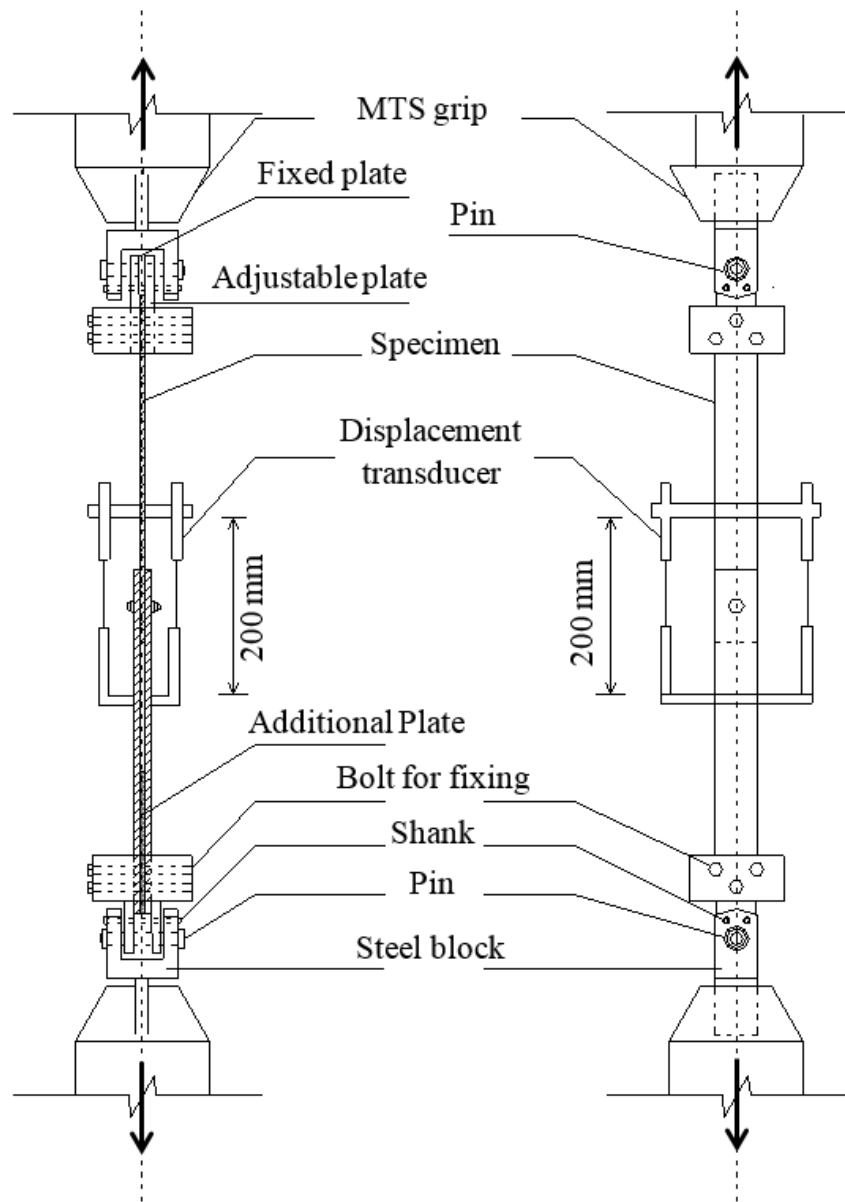


**Fig. 5.** Schematic view of test setup for TSS double shear bolted connection

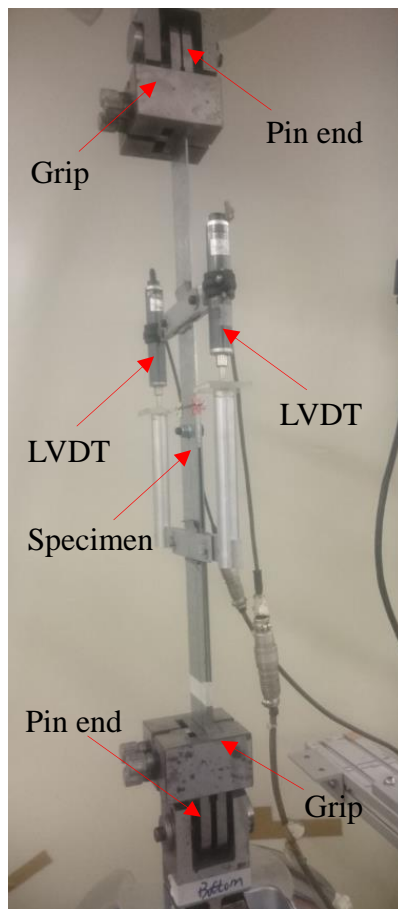


**Fig. 6.** Test setup of TSS double shear bolted connection

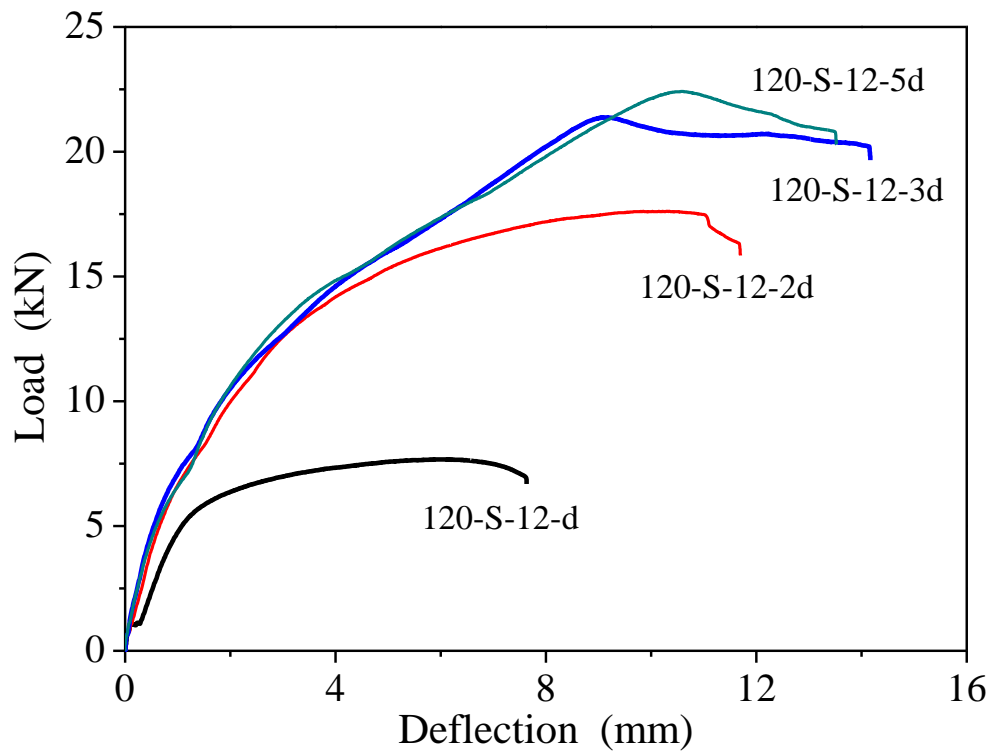


**Fig. 7.** Load-deflection curves of TSS specimen Series 120-S-12

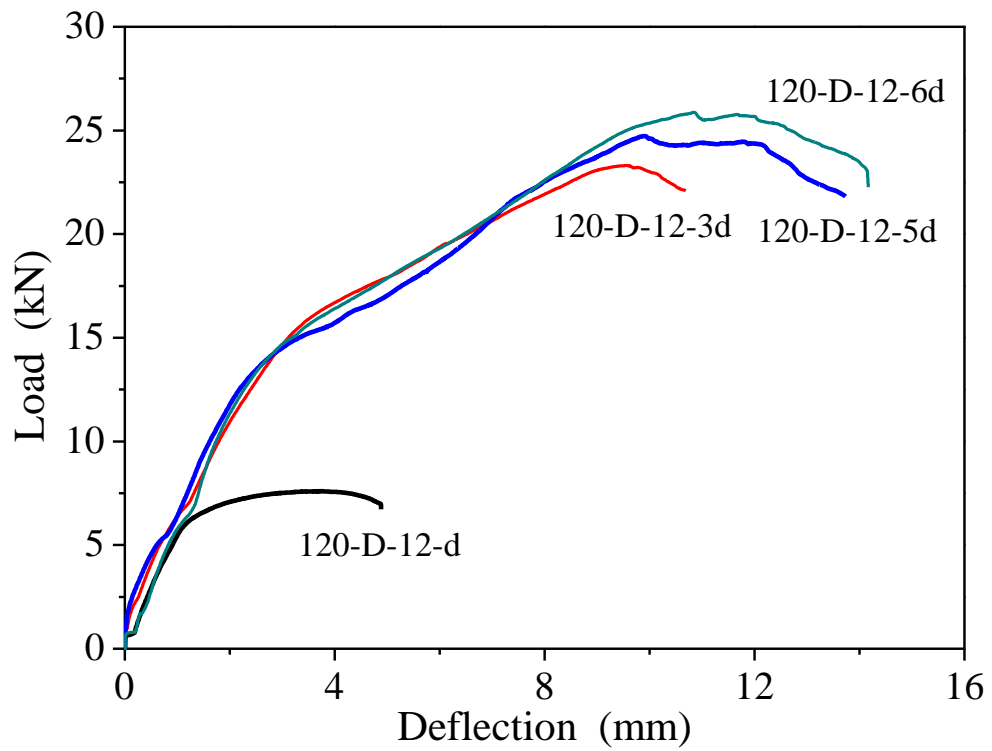


**Fig. 8.** Load-deflection curves of TSS specimen Series 120-D-12

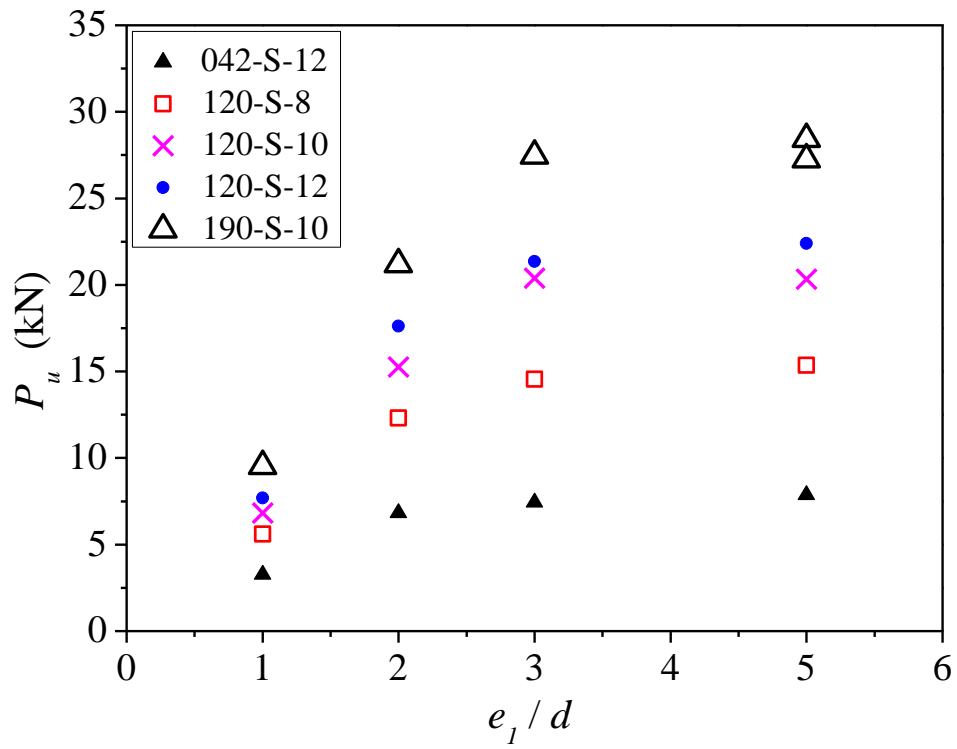


**Fig. 9.** Effects of end distance on ultimate load of TSS single shera bolted connections

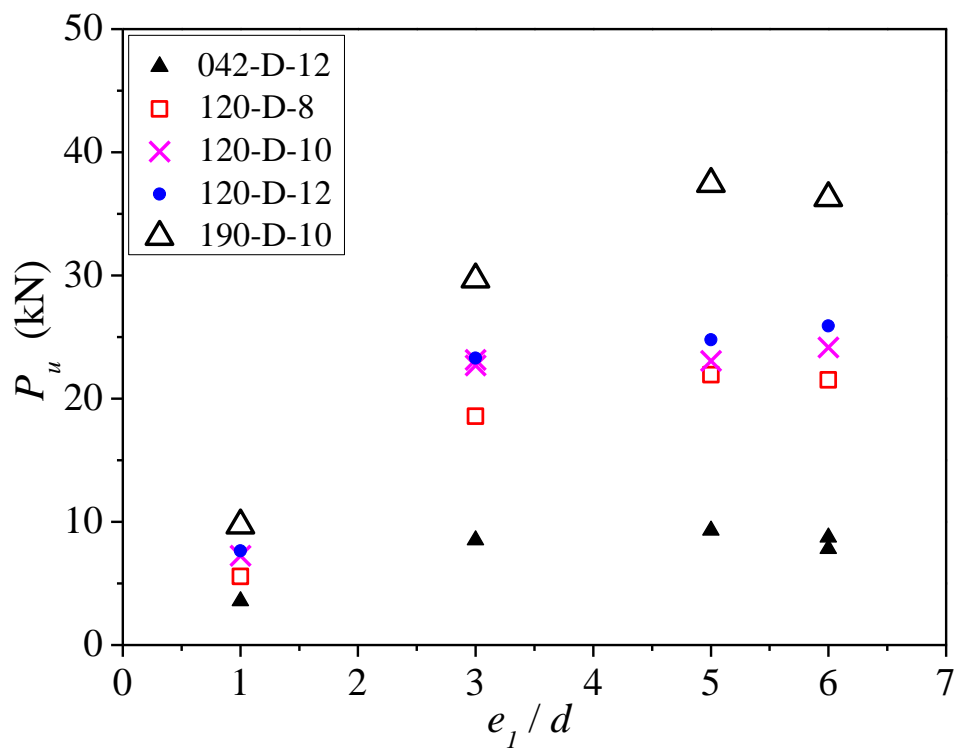
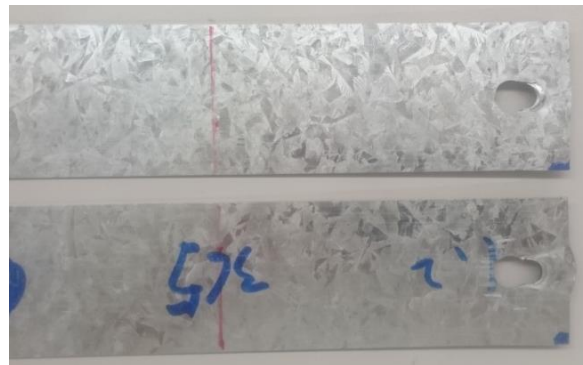


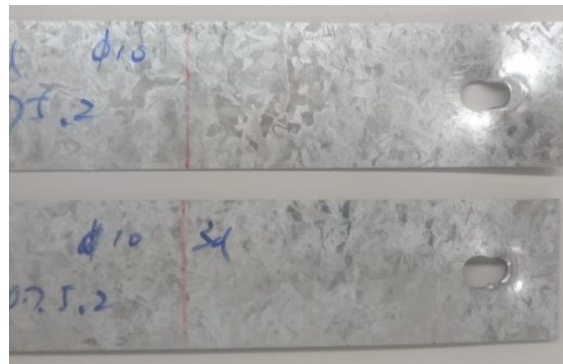
**Fig. 10.** Effects of end distance on ultimate load of TSS double shera bolted connections



(a) 120-S-10-d



(b) 120-S-10-2d



(c) 120-S-10-3d



(d) 120-S-10-5d

**Fig. 11.** Failure modes of TSS specimen Series 120-S-10



(a) 190-S-10-d



(b) 190-S-10-2d

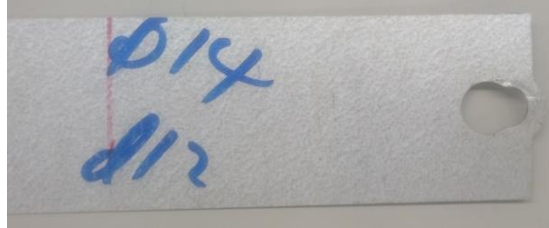


(c) 190-S-10-3d



(d) 190-S-10-5d

**Fig. 12.** Failure modes of TSS specimen Series 190-S-10



(a) 042-D-12-d



(b) 042-D-12-3d

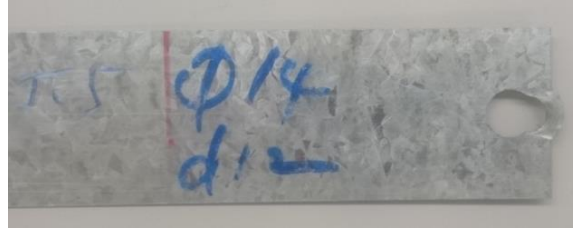


(c) 042-D-12-5d

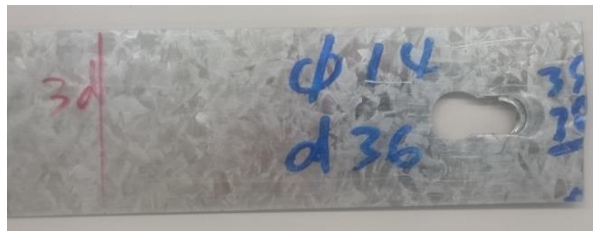


(d) 042-D-12-6d

**Fig. 13.** Failure modes of TSS specimen Series 042-D-12



(a) 120-D-12-d



(b) 120-D-12-3d

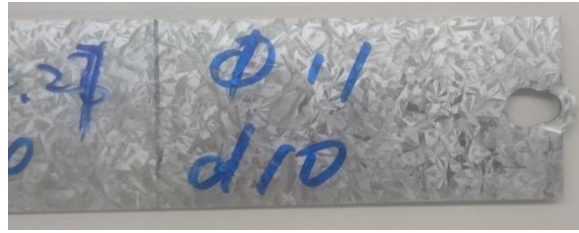


(c) 120-D-12-5d

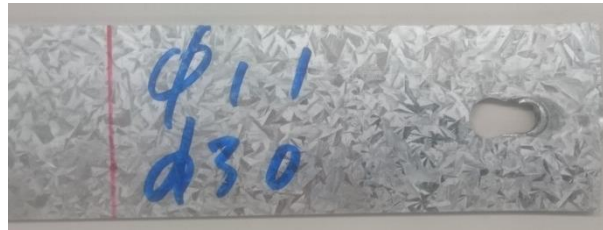


(d) 120-D-12-6d

**Fig. 14.** Failure modes of TSS specimen Series 120-D-12



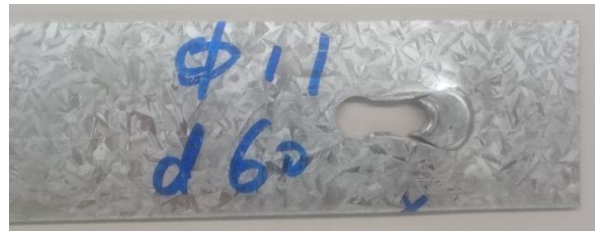
(a) 190-D-10-d



(b) 190-D-10-3d



(c) 190-D-10-5d



(d) 190-D-10-6d

**Fig. 15.** Failure modes of TSS specimen Series 190-D-10

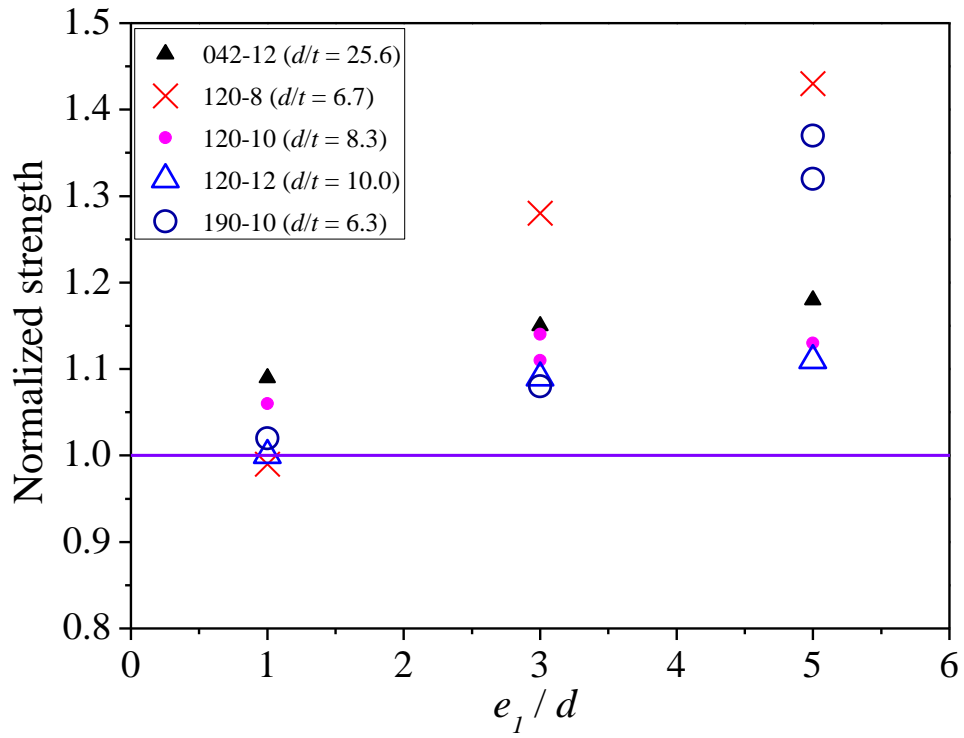


**Fig. 16.** Ultimate strengths of double shear normalized by those of single shear for the same bolt hole and end distance

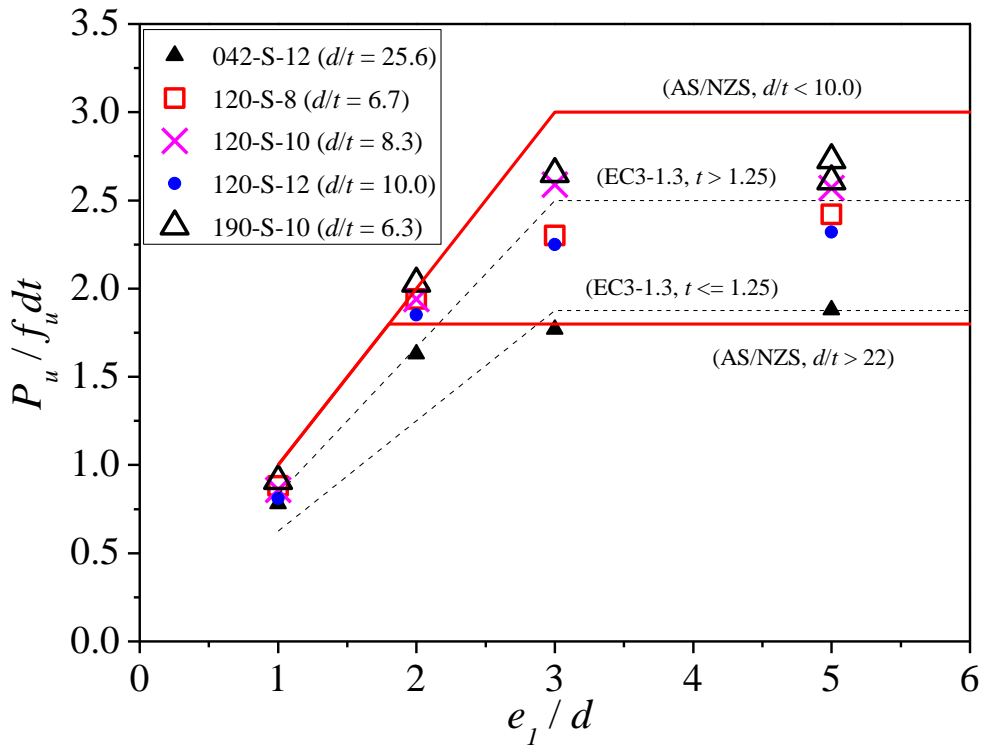


Fig. 17. Comparison of test strengths with predictions for single shear bolted connections

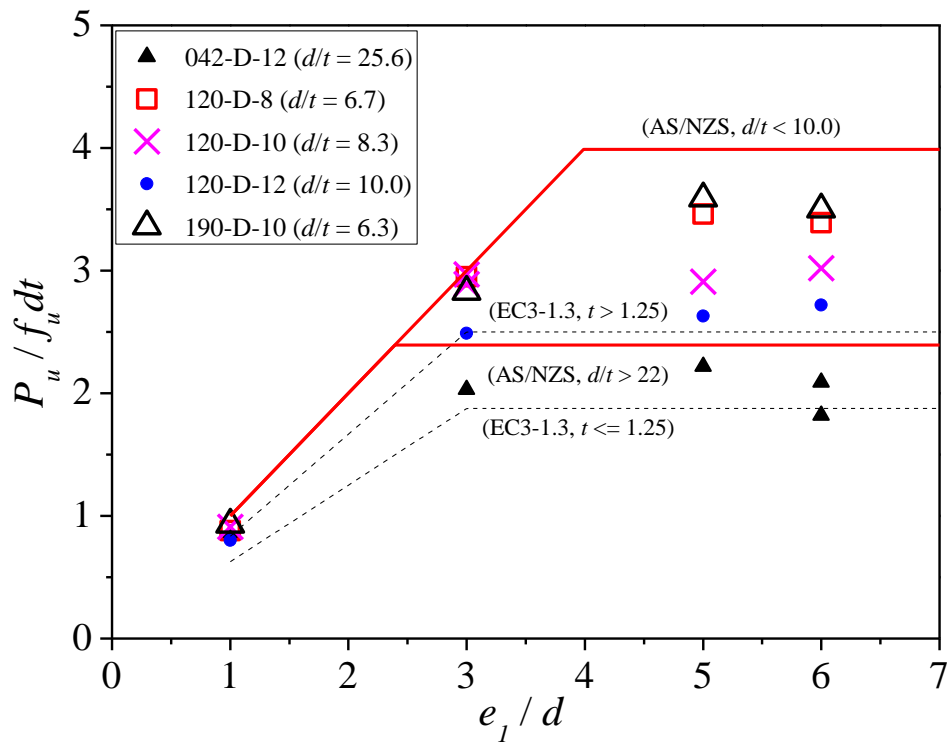


Fig. 18. Comparison of test results with predictions for double shear bolted connections

Steel grade	$t_m$ (mm)	$w_m$ (mm)	$E$ (GPa)	$f_{0.2}$ (MPa)	$f_u$ (MPa)	$\varepsilon_u$ (%)	$\varepsilon_f$ (%)
G550	0.41	6.04	228	730	743	0.5	2.9
G500	1.18	5.98	220	622	633	3.8	9.2
G450	1.83	6.03	213	512	543	7.2	15.9

**Table 1** Material properties of TSS

Bolt type	Normal diameter (mm)	Measured diameter (mm)
M8	8.0	7.8
M10	10.0	9.8
M12	12.0	11.9

**Table 2** Details of steel bolts

Washer type	Inner diameter (mm)	Outside diameter (mm)	Thickness (mm)
M8	8.46	22.00	1.68
M10	10.48	24.98	1.34
M12	13.17	23.76	1.18

**Table 3** Details of steel washers

Codes	$e_1$	$e_2$
AS/NZS [11]	$\geq 1.5d$	$\geq 1.5d$
NAS [12]	$\geq 1.5d$	$\geq 1.5d$
EC3-1.3 [13]	$\geq 1.0d_o$	$\geq 1.5d_o$

**Table 4** Spacing requirements for bolt connections in different codes

Connection type	Steel grade	$t$ (mm)	$d$ (mm)	$e_1$
Single shear	G550	0.42	12	$1.0d, 2.0d, 3.0d$ and $5.0d$
	G500	1.20	8, 10 and 12	
	G450	1.90	10	
Double shear	G550	0.42	12	$1.0d, 3.0d, 5.0d$ and $6.0d$
	G500	1.20	8, 10 and 12	
	G450	1.90	10	

**Table 5** Design of TSS one-bolted connection specimens

Specimen	$t_m$ (mm)	$d/t_m$	$P_u$ (kN)	$P_u/P_{AS/NZS}$	$P_u/P_{NAS}$	$P_u/P_{EC}$
042-S-12-d	0.47	25.53	3.27	0.78 (1.41) <sup>#</sup>	1.56 (2.72) <sup>#</sup>	1.25
042-S-12-2d	0.47	25.53	6.82	0.90 (1.64) <sup>#</sup>	0.96 (1.67) <sup>#</sup>	1.30
042-S-12-3d	0.47	25.53	7.43	0.99 (1.79) <sup>#</sup>	0.99 (1.71) <sup>#</sup>	0.95
042-S-12-5d	0.47	25.53	7.87	1.04 (1.89) <sup>#</sup>	1.04 (1.82) <sup>#</sup>	1.00
120-S-8-d	1.25	6.40	5.60	0.88	1.68 (1.87) <sup>#</sup>	1.06
120-S-8-2d	1.25	6.40	12.30	0.97	1.12 (1.25) <sup>#</sup>	1.16
120-S-8-3d	1.25	6.40	14.56	0.77	0.79 (0.87) <sup>#</sup>	0.92
120-S-8-5d	1.25	6.40	15.35	0.81	0.81 (0.90) <sup>#</sup>	0.97
120-S-10-d	1.25	8.00	6.82	0.86	1.59 (1.77) <sup>#</sup>	1.03
120-S-10-2d	1.24	8.06	15.26	0.97	1.12 (1.24) <sup>#</sup>	1.17
120-S-10-3d	1.24	8.06	20.39	0.86	0.88 (0.98) <sup>#</sup>	1.04
120-S-10-5d	1.25	8.00	20.34	0.86	0.86 (0.95) <sup>#</sup>	1.03
120-S-12-d	1.25	9.60	7.68	0.81	1.62 (1.79) <sup>#</sup>	0.97
120-S-12-2d	1.25	9.60	17.62	0.93	1.09 (1.21) <sup>#</sup>	1.11
120-S-12-3d	1.25	9.60	21.35	0.88	0.81 (0.90) <sup>#</sup>	0.90
120-S-12-5d	1.27	9.45	22.40	0.91	0.84 (0.93) <sup>#</sup>	0.93
190-S-10-d	1.92	5.21	9.53	0.91	1.69	1.10
190-S-10-2d	1.92	5.21	21.20	1.02	1.17	1.22
190-S-10-3d	1.91	5.24	27.47	0.88	0.90	1.06
190-S-10-5d	1.92	5.21	28.44	0.91	0.91	1.09
190-S-10-5d-r	1.92	5.21	27.25	0.87	0.87	1.05
Steel 0.42 mm G550			<b>Mean</b>	0.93 (1.68) <sup>#</sup>	1.14 (1.98) <sup>#</sup>	1.12
			<b>COV</b>	0.123 (0.123) <sup>#</sup>	0.251 (0.251) <sup>#</sup>	0.157
Steel 1.20 mm G500			<b>Mean</b>	0.88	1.10 (1.22) <sup>#</sup>	1.02
			<b>COV</b>	0.072	0.312 (0.312) <sup>#</sup>	0.089
Steel 1.90 mm G450			<b>Mean</b>	0.92	1.11	1.10
			<b>COV</b>	0.063	0.314	0.063

Note: (x)<sup>#</sup> result by using reduced material properties.

**Table 6** Test strengths and comparisons for TSS single shear bolted connections

Specimen	$t_m$ (mm)	$d/t_m$	$P_u$ (kN)	$P_u/P_{AS/NZS}$	$P_u/P_{NAS}$	$P_u/P_{EC}$
042-D-12-d	0.47	25.53	3.56	0.85 (1.54) <sup>#</sup>	1.70 (2.96) <sup>#</sup>	1.36
042-D-12-3d	0.47	25.53	8.52	0.85 (1.54) <sup>#</sup>	0.85 (1.48) <sup>#</sup>	1.08
042-D-12-5d	0.47	25.53	9.29	0.93 (1.68) <sup>#</sup>	0.93 (1.61) <sup>#</sup>	1.18
042-D-12-6d	0.48	25.00	7.81	0.76 (1.38) <sup>#</sup>	0.76 (1.33) <sup>#</sup>	0.97
042-D-12-6d-r	0.47	25.53	8.74	0.87 (1.58) <sup>#</sup>	0.87 (1.52) <sup>#</sup>	1.11
120-D-8-d	1.24	6.45	5.55	0.88	1.68 (1.87) <sup>#</sup>	1.06
120-D-8-3d	1.24	6.45	18.57	0.98	1.01 (1.12) <sup>#</sup>	1.18
120-D-8-5d	1.25	6.40	21.95	0.87	0.87 (0.96) <sup>#</sup>	1.38
120-D-8-6d	1.25	6.40	21.52	0.85	0.85 (0.95) <sup>#</sup>	1.36
120-D-10-d	1.25	8.00	7.25	0.91	1.68 (1.88) <sup>#</sup>	1.10
120-D-10-3d	1.23	8.13	23.16	0.99	1.01 (1.12) <sup>#</sup>	1.20
120-D-10-3d-r	1.24	8.06	22.69	0.96	0.98 (1.09) <sup>#</sup>	1.16
120-D-10-5d	1.25	8.00	23.07	0.88	0.81 (0.90) <sup>#</sup>	1.16
120-D-10-6d	1.26	7.94	24.16	0.91	0.84 (0.94) <sup>#</sup>	1.21
120-D-12-d	1.25	9.60	7.65	0.80	1.61 (1.79) <sup>#</sup>	0.97
120-D-12-3d	1.23	9.76	23.30	0.98	0.90 (1.00) <sup>#</sup>	1.00
120-D-12-5d	1.24	9.68	24.77	1.03	0.95 (1.05) <sup>#</sup>	1.05
120-D-12-6d	1.25	9.60	25.91	1.07	0.98 (1.09) <sup>#</sup>	1.09
190-D-10-d	1.92	5.21	9.72	0.93	1.73	1.12
190-D-10-3d	1.93	5.18	29.68	0.94	0.96	1.13
190-D-10-5d	1.92	5.21	37.45	1.08	1.00	1.44
190-D-10-6d	1.91	5.24	36.29	1.06	0.98	1.40
Steel 0.42 mm G550			<b>Mean</b>	0.85 (1.54) <sup>#</sup>	1.02 (1.78) <sup>#</sup>	1.14
			<b>COV</b>	0.069 (0.069) <sup>#</sup>	0.375 (0.375) <sup>#</sup>	0.126
Steel 1.20 mm G500			<b>Mean</b>	0.93	1.09 (1.21) <sup>#</sup>	1.15
			<b>COV</b>	0.082	0.304 (0.304) <sup>#</sup>	0.108
Steel 1.90 mm G450			<b>Mean</b>	1.00	1.17	1.27
			<b>COV</b>	0.077	0.320	0.133

Note: (x)<sup>#</sup> result by using reduced material properties.

**Table 7** Test strengths and comparisons for TSS double shear bolted connections

Connection type	No. of tests		$P_u/P_{AS/NZS}$	$P_u/P_{NAS}$	$P_u/P_{EC}$
Single shear	21	Mean, $P_m$	0.90	1.11	1.06
		COV, $V_p$	0.082	0.287	0.105
		Resistance factor, $\phi$	0.60 (0.60)*	0.60	0.80 (0.60)*
		Reliability index, $\beta$	3.49 (3.71)*	2.92	2.96 (4.23)*
Double shear	22	Mean, $P_m$	0.93	1.09	1.17
		COV, $V_p$	0.092	0.309	0.119
		Resistance factor, $\phi$	0.60 (0.60)*	0.60	0.80 (0.60)*
		Reliability index, $\beta$	3.57 (3.78)*	2.75	3.24 (4.48)*

Note: (x)\* result by using load combination of 1.2DL + 1.6LL.

**Table 8** Summary of test strengths compared with predictions from design specifications

Specimens	Test	AS/NZS [11]	NAS [12]	EC3-1.3 [13]
042-S-12-d	T	T	T	B
042-S-12-2d	T	B	T	B
042-S-12-3d	B	B	B	B
042-S-12-5d	B	B	B	B
120-S-8-d	T	T	T	B
120-S-8-2d	T	T	T	B
120-S-8-3d	B	T + B	T	B
120-S-8-5d	B	B	B	B
120-S-10-d	T	T	T	B
120-S-10-2d	T	T	T	B
120-S-10-3d	B	T + B	T	B
120-S-10-5d	B	B	B	B
120-S-12-d	T	T	T	B
120-S-12-2d	T	T	T	B
120-S-12-3d	B	NS	NS	B
120-S-12-5d	B	NS	NS	B
190-S-10-d	T	T	T	B
190-S-10-2d	T	T	T	B
190-S-10-3d	B	T + B	T	B
190-S-10-5d	B	B	B	B
190-S-10-5d-r	B	B	B	B

T = Tearout (shear fracture), B = Bearing failure; NS = Net section tension (shear fracture).

**Table 9** Failure modes of TSS single shear bolted connections

Specimens	Test	AS/NZS [11]	NAS [12]	EC3-1.3 [13]
042-D-12-d	T	T	T	B
042-D-12-3d	T	B	B	B
042-D-12-5d	B	B	B	B
042-D-12-6d	B	B	B	B
042-D-12-6d-r	B	B	B	B
120-D-8-d	T	T	T	B
120-D-8-3d	T	T	T	B
120-D-8-5d	B	B	B	B
120-D-8-6d	B	B	B	B
120-D-10-d	T	T	T	B
120-D-10-3d	T	T	T	B
120-D-10-3d-r	T	T	T	B
120-D-10-5d	B	NS	NS	B
120-D-10-6d	B	NS	NS	B
120-D-12-d	T	T	T	B
120-D-12-3d	T	NS	NS	B
120-D-12-5d	B	NS	NS	B
120-D-12-6d	B	NS	NS	B
190-D-10-d	T	T	T	B
190-D-10-3d	T	T	T	B
190-D-10-5d	B	NS	NS	B
190-D-10-6d	B	NS	NS	B

**Table 10** Failure modes of TSS double shear bolted connections